Hyper Rayleigh Scattering from DNA Nucleotides in Aqueous Solution

Christian Jonin, Maksymilian Dereniowski, Estelle Salmon, Csilla Gergely, Katarzyna Matczyszyn, Pierre-François Brevet

▶ **To cite this version:**

Christian Jonin, Maksymilian Dereniowski, Estelle Salmon, Csilla Gergely, Katarzyna Matczyszyn, et al.. Hyper Rayleigh Scattering from DNA Nucleotides in Aqueous Solution. Journal of Chemical Physics, 2023, 159, pp.054303. 10.1063/5.0155821 . hal-04163438

HAL Id: hal-04163438
https://hal.science/hal-04163438

Submitted on 17 Jul 2023

HAL is a multi-disciplinary open access archive for the deposit and dissemination of scientific research documents, whether they are published or not. The documents may come from teaching and research institutions in France or abroad, or from public or private research centers.

L'archive ouverte pluridisciplinaire **HAL**, est destinée au dépôt et à la diffusion de documents scientifiques de niveau recherche, publiés ou non, émanant des établissements d'enseignement et de recherche français ou étrangers, des laboratoires publics ou privés.

Hyper Rayleigh Scattering from DNA Nucleotides in Aqueous Solution

Christian Jonin[1], Maksymilian Dereniowski[3], Estelle Salmon[2], Csilla Gergely[1],

Katarzyna Matczyszyn[3] and Pierre-François Brevet[2]

[1] *Laboratoire Charles Coulomb, Univ. Montpellier, CNRS, Montpellier, France*

[2]*Institut Lumière Matière, UMR CNRS 5306, Université Claude Bernard Lyon 1, 10 Rue Ada Byron, 69622 Villeurbanne Cedex, France.*

[3]Advanced Materials Engineering and Modeling Group, Wroclaw University of Science and Technology, Wroclaw, Poland.

Corresponding Author : Christian Jonin, christian.jonin@umontpellier.fr

ABSTRACT

Nucleotides are organic compounds consisting of a phosphate group, a nitrogenous base, namely adenine (A), thymine (T), cytosine (C), or guanine (G), and a sugar, here deoxyribose. The magnitude of the first hyperpolarizability β of these four DNA nucleotides were determined in aqueous solution with the nonlinear optical technique of Hyper Rayleigh Scattering under non resonant conditions at the fundamental wavelength of 800 nm. The smallest value is found to be $1.67 \pm 0.15 \times 10^{-30}$ esu for thymidine-5'-monophosphate and the highest is $1.76 \pm 0.16 \times 10^{-30}$ esu for 2'-guanosine-5'-monophosphate. Polarization resolved studies were also performed to question the symmetry of the first hyperpolarizability tensor and access the ratio of some elements of the first hyperpolarizability tensor.

These experimental results were then compared to theoretical values of these first hyperpolarizabilities obtained with the Density Functional Theory at the level of the PCM-B3LYP/6-31G+(d) basis and taking into account the solvent.

INTRODUCTION

The nonlinear optical technique of Hyper Rayleigh Scattering (HRS) is an efficient method to determine the first hyperpolarizability of molecular compounds and nanoparticles in solution.[1] These measurements allow for the characterization of the solute quadratic optical nonlinear response and, in the case of macromolecules containing more than one nonlinear optical chromophore, can yield information about the macromolecular conformation in solution.[2] HRS is the incoherent second-order light scattering process occurring in isotropic bulk solutions due to fluctuations of the molecular orientation.[3] The HRS technique has been introduced in 1991 and has since then been extensively used to measure the first hyperpolarizability of a variety of solutes,[4,5] including ionic species,[6,7] octupolar molecules[8,9] or push-pull compounds designed for optoelectronic devices.[10,11] Studies of biomolecules by HRS concerned initially the bacteriorhodopsin protein contained in purple membranes and its retinal chromophore and collagen but has since been largely extended.[13-16]. The angular dependence of the HRS intensity from a suspension of purple membranes was also monitored in order to unravel further information on the nonlinear response symmetry.[17,18]

In-depth knowledge of DNA and RNA structure forms the basis for research on gene expression mechanisms. Also, the refinement of three-dimensional models of DNA and RNA structure are strongly associated with advances in the structural chemistry of nucleic acids. It is absolutely clear that three-dimensional models of the structure of synthetic and natural polynucleotides can be constructed and correctly interpreted only with a profound knowledge of the conformation of monomer components of nucleic acids, i.e. nucleosides and nucleotides.

Beyond nucleotides, in-depth knowledge of DNA structure forms the basis of an active research field. Structural polymorphism of DNA has been evolving since the double helical model and non-canonical DNA structures have constantly been documented, see for instance

hairpins, cruciforms, triplex, G-triplexes, quadruplexes or i-motifs to name a few[19-20]. Many of the non-canonical structures have shown their involvement in diseases like cancer and genetic disorders [21]. Therefore, aiming towards methodologies identifying those non-canonical structures remains of interest and the present work constitutes a first step into this direction.

In this paper, we further extend these studies to biological materials in reporting the measurement of the first hyperpolarizability of the four DNA nucleotides and compare them to the results of DFT calculations at the PCM-B3LYP/6-31+G(d) basis level. A polarization analysis of the HRS intensity was also performed to question the symmetry of the first hyperpolarizability tensor. This work presents a complementary study to our previous work where the first hyperpolarizability of the DNA bases in water was determined.[22]

EXPERIMENTAL SECTION

HRS Apparatus. The experimental HRS setup used in this study to determine the solute hyperpolarizability has already been described elsewhere.[22-25] Briefly, the output of a femtosecond Ti:Sapphire laser with a pulse duration of 180 fs at a wavelength of 800 nm was used to generate incoherent scattered light at the harmonic frequency from the sample cell. In order to control the energy per pulse of the light impinging onto the sample, the beam was passed through a half wave plate followed by a polarizing cube. By rotating the half wave plate keeping the polarizer in a fixed position, the energy of the fundamental light could be varied. The typical fundamental beam energy used was in the range of 0.5 nJ per pulse. The fundamental beam was linearly polarized and its angle of polarization defined with a second half-wave plate placed after the polarizing cube. Any spurious second harmonic light was then filtered out and the laser beam was gently focused using a microscope objective (X16, NA = 0.32) into the sample cell. After passing through the cell, the fundamental beam was

carefully dumped and the collection of the blue second-harmonic light at 400 nm was performed at right angle. This second-harmonic scattered light was collected with a lens and then, through the spectrometer. For the polarization resolved experiments, a half-wave plate and a polarizing cube are used to select the vertical or horizontal polarization. It has to be noted that the maximum transmission through the spectrometer is obtained for a signal with a vertical polarization. Then, the polarizing cube allows us to preserve the vertical polarization while the half-wave plate can be turn to select either the output vertical or horizontal polarization. A 25 mm focal length lens was placed at the entrance of a spectrometer to obtain the maximum intensity into the CCD camera.

Hyperpolarizability determination: The experimental procedure for the determination of the first hyperpolarizability magnitude was the following. We used the external reference method where the power dependence of the HRS intensity from the sample and a reference compound are determined. In the present study, the reference sample was simply neat water, the first hyperpolarizability of which is taken as $\beta_W = \sqrt{\langle \beta_W^2 \rangle} = 0.087 \times 10^{-30}$ esu.[23] Here, $\langle \beta_W^2 \rangle$ stands for the square of the first hyperpolarizability of water averaged over all spatial molecular orientation. The subscript *W* indicates neat water. This first hypolarizability value assumes that the measurement is performed for vertically polarized fundamental light and no polarization selection on the harmonic scattered light. For the solvent, the HRS intensity then writes as :

$$I_{HRS} = G N_W \langle \beta_W^2 \rangle \, I_\omega^2 \qquad (1)$$

where N_W is the concentration, namely 55.56 M, I_ω is the fundamental beam intensity and G a general constant accounting for all other parameters. In presence of the nucleotides in the solution, Eq.(1) must be rewritten as :

$$I_{HRS} = G[N_W\langle\beta_W^2\rangle + N_i\langle\beta_i^2\rangle]I_\omega^2 \quad (2)$$

to account for the presence of both the nucleotides and the solvent. Here, the subscript *i* stands for the nucleotides. Hence, a simple power dependence study of the sample and the reference allows to extract from the slope of the line plots of the HRS intensity as a function of the square of the fundamental intensity the sample first hyperpolarizability as $\sqrt{\langle\beta_i^2\rangle}$. During all acquisitions, the measured HRS intensity was normalized with respect to the square of the incident power impinging on the cell to account for temporal fluctuations in the laser power. Care was also exercised to ensure that the intercept of the line plot coincided with vanishing intensity at vanishing fundamental intensity.

Chemicals. Neat water obtained by reverse osmosis followed by ion exchange (Millipore, Milli-Q SP reagent system) was used throughout. Commercially available 2'-deoxycytidine-5'-monophosphate disodium salt (Alfa Aesar, dCMP), 2'-deoxyguanosine-5'-monophosphate disodium salt hydrate, 98% purity (Alfa Aesar, dGMP), 2'-deoxyadenosine-5'-monophosphate, 98% purity (Alfa Aesar, dAMP) and 2'-deoxythymidine-5'-monophosphate disodium salt (Alfa Aesar, dTMP) were used. Additionally, 1 M NH_4OH aqueous solution was used for 2'-deoxyadenosine-5'-monophosphate as solvent instead of neat water due to its low solubility. All bases were thus highly soluble in their respective solvent as compared to the case of the nucleobases reported previously.[22] Solutions of 0.2 M of the four nucleotides were thus prepared. No difference in HRS intensity was detected in these measurements

between neat water and the neat 1 M NH_4OH aqueous solution supporting the use of the first hyperpolarizability of neat water as the reference. Likewise, the first hyperpolarizability of the hydrated counterions was founds negligible and thus the first hyperpolarizability determined is that of the nucleotides only.

RESULTS AND DISCUSSION

DNA Nucleotides. The first hyperpolarizability of the four DNA nucleotides was determined from HRS measurements using the procedure described above. To ensure that the signal recorded was indeed an HRS signal, a spectrum around the HRS line at the harmonic frequency was recorded to ensure that no spurious light was collected apart the HRS line at 400 nm, see Figure 1(a). Then, the quadratic dependence with the fundamental beam intensity of the HRS intensity, extracted from Figure 1(a) as the amplitude of the Gaussian profile of the HRS line, was obtained for neat water, see Figure 1(b). For simplicity, the fundamental intensity was replaced with the average fundamental power P_ω for commodity, and likewise subsequently.

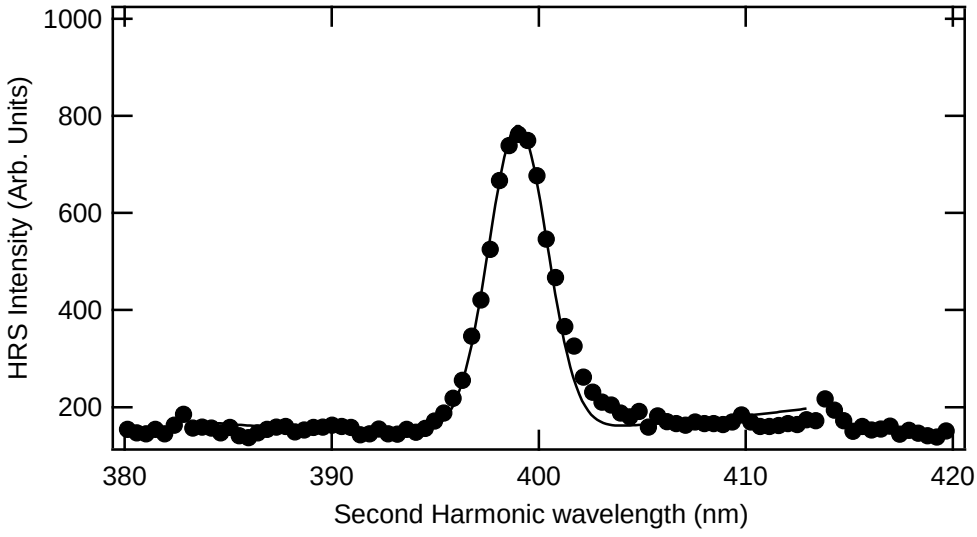

(a)

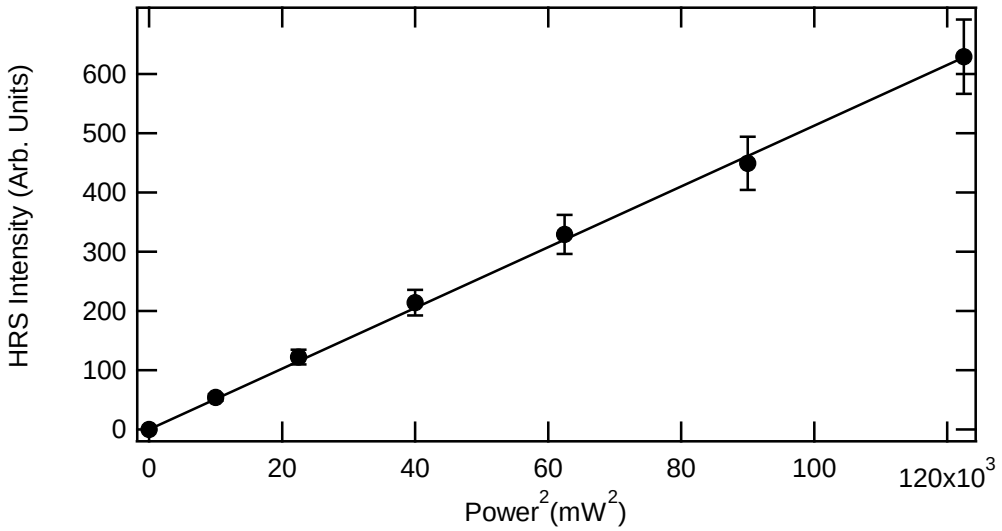

(b)

Figure 1 : (a) Spectrum of the HRS intensity at 400 nm for neat water using a 300 mW laser incident power for the 800 nm wavelength fundamental beam (markers). Full line represents a Gaussian fit, (b) Dependence of the HRS intensity from neat water with the square of the fundamental intensity, (markers) experimental data, (dashed line) adjustment with a linear plot.

Then, the dependence of the HRS intensity for the four nucleotides was recorded as a function of the fundamental beam intensity. Figure 2 presents the result for the HRS intensity from the dAMP solution as a function of the square of the fundamental intensity. A linear plot going through the origin is obtained as expected.

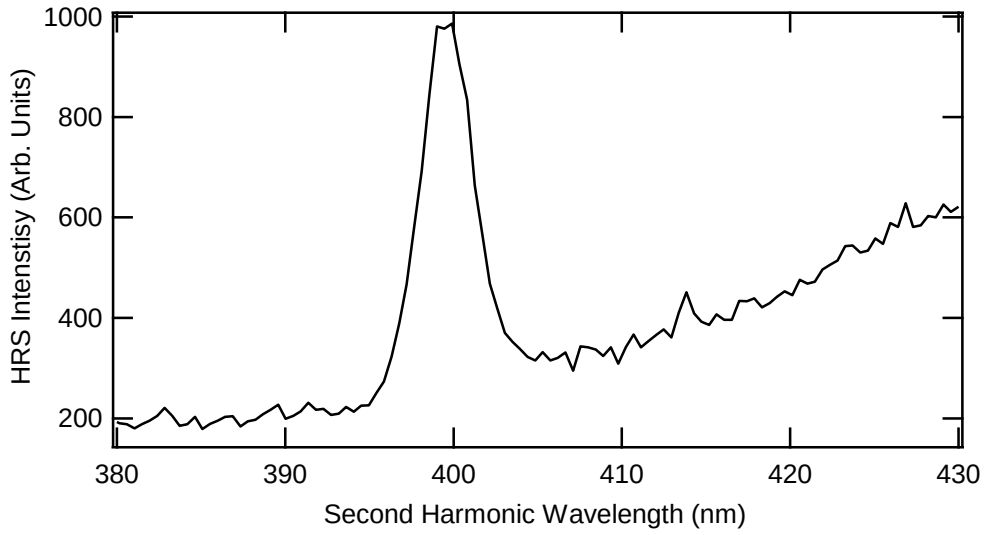

(a)

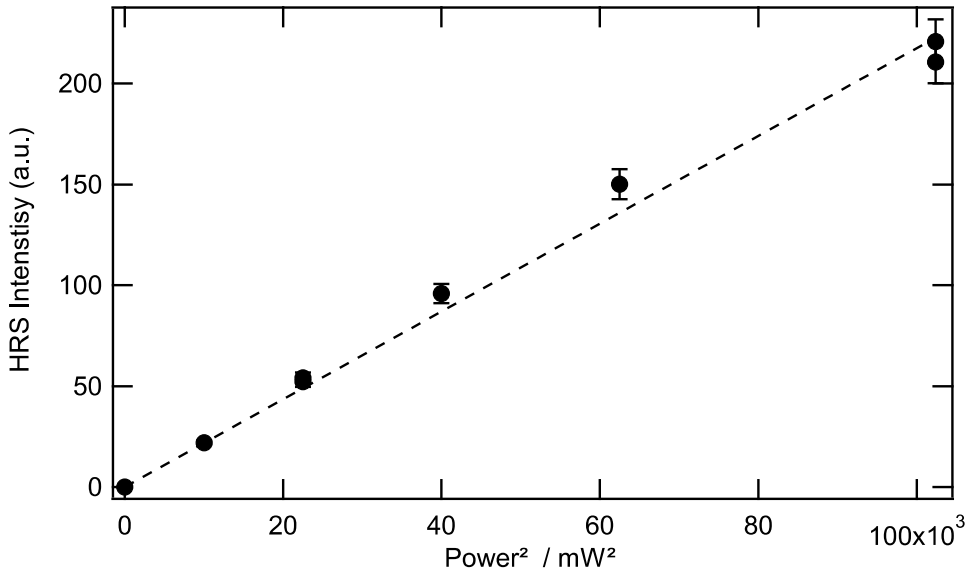

(b)

Figure 2 : (a) Spectrum of the HRS intensity at 400 nm of a 0.2 M dAMP aqueous solution for a 315 mW laser incident power for a 800 nm wavelength fundamental beam. (b) Dependence of the HRS intensity from the 0.2 M dAMP aqueous solution with the square of the fundamental average power, (markers) experimental data, (dashed line) adjustment with a linear plot.

From Figures 1 and 2, the dAMP first hyperpolarizability was determined to be $(1.70 \pm 0.2) \times 10^{-30}$ esu. Units are given in esu for convenience with respect to the available litterature. However, to report first hyperpolarizabilities in the international system of units, that is in units of $C.m^3.V^{-2}$, values in esu units must be multiplied by the factor $4\pi\varepsilon_0/3 \times 10^{10}$. Experiments were repeated twice and the average dAMP first hyperpolarizability value is given above. This first hyperpolarizability was determined under non-resonant HRS conditions. Indeed, all nucleotides absorb in the UV region, around about 260 nm. Thus neither the fundamental wavelength at 800 nm nor the harmonic wavelength at 400 nm are in resonance to any absorption bands.

However, on the long wavelength side of the HRS line, the onset of a broad photoluminescence band is observed, likely resulting from multiphoton excitation. This background can be subtracted from the HRS intensity line using the spectral domain method [23] with an expression resulting from the simple superposition of a Gaussian profile and a second order polynomial. This subtraction procedure is possible because the two signals are incoherent and no interferences can occur between them. Then, at the fixed wavelengths of 420 nm away from the HRS line and 400 nm for the HRS line itself, the collected intensity was plotted as a function of the input fundamental intensity in a log-log plot, see Figure S1 in the Supplementary Information file. As expected, the HRS intensity follows a square dependence with the input fundamental intensity, as indicated by a slope of 2 in the log-log plot. On the opposite, the photoluminescence appears with a larger slope in this log-log plot indicating that the photo-excitation step involves two and three photons processes. Not surprisingly, double ring nucleotides dAMP and dGMP indeed exhibits photoluminescence whereas single ring dTMP and dCMP do not. This feature likely results from the higher photon energy required to achieve photo-excitation in single ring nucleotides, considering that the onset of absorption lies at about 260 nm.

Similar measurements were then performed for 2'-deoxycytidine-5'-monophosphate (dCMP), see Figure 3.

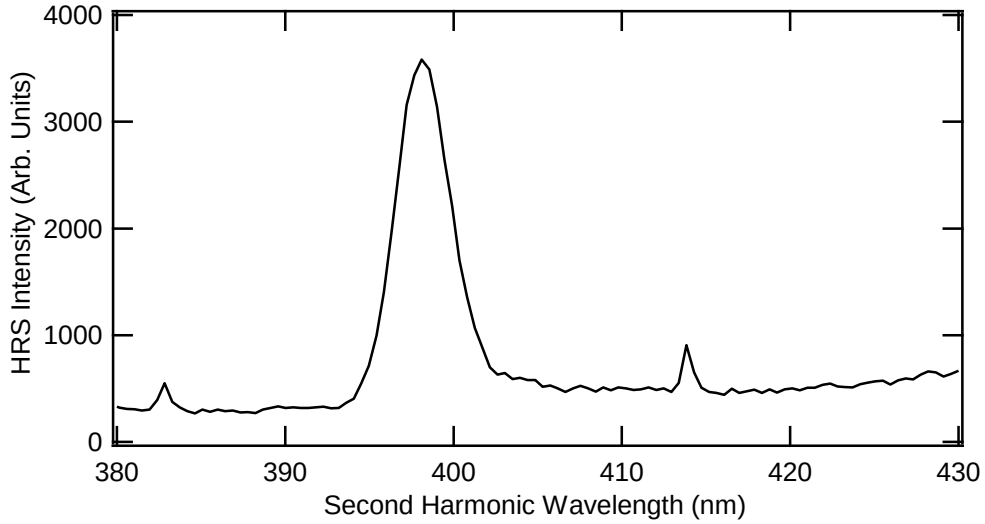

(a)

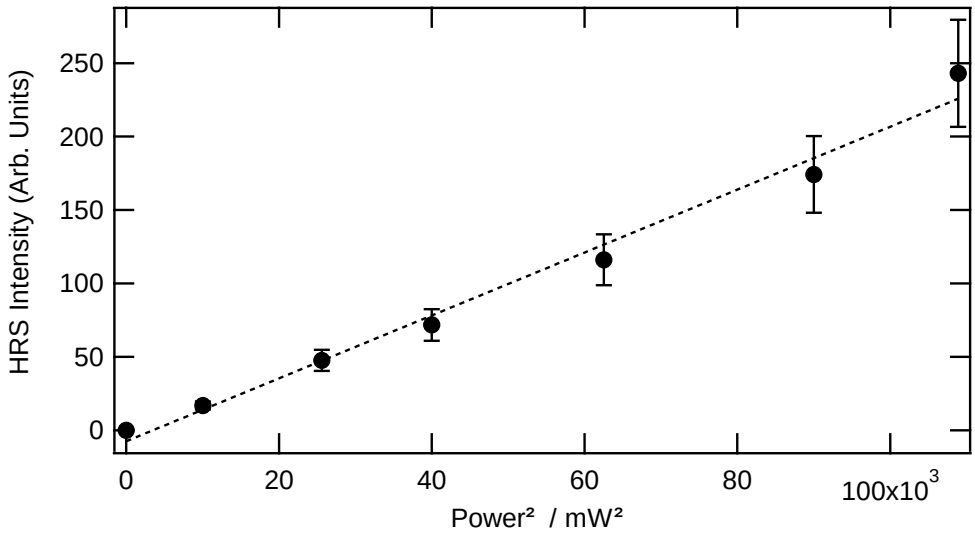

(b)

Figure 3 : (a) Spectrum of the HRS intensity of the 0.2M dCMP aqueous solution for a 315 mW laser incident power at 400 nm for a 800 nm fundamental beam wavelength. (b)

Dependence of the 0.2 M dCMP aqueous solution with the square of the fundamental average power, (markers) experimental data, (dashed line) adjustment with a linear plot.

The HRS intensity with the square of the fundamental intensity displays the expected linear behavior too. The dCMP first hyperpolarizability obtained from averaging the results of two experiments is $(1.5 \pm 0.2) \times 10^{-30}$esu. Figure 4 reports the results for deoxythymidine-5'-monophosphate dTMP.

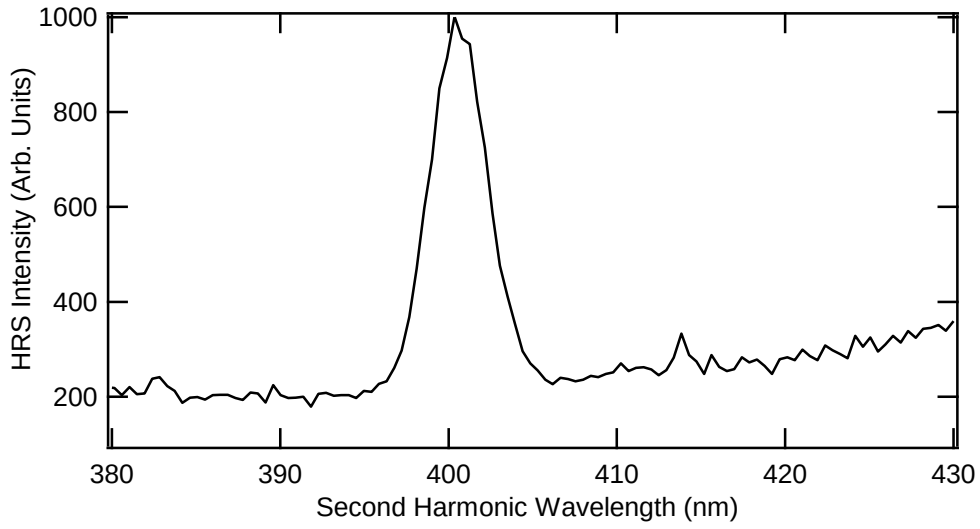

(a)

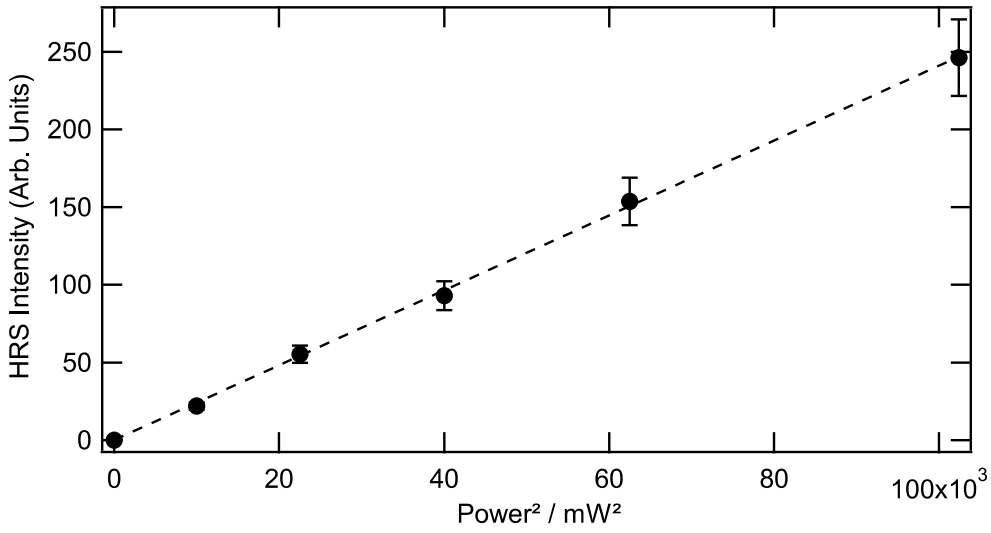

(b)

Figure 4 : (a) Spectrum of the HRS intensity at 400 nm of the 0.2 M dTMP aqueous solution for a 320 mW laser incident power for a 800 nm wavelength fundamental beam. (b) Dependence of the HRS intensity of the 0.2 M dTMP aqueous solution with the square of the fundamental average power, (markers) experimental data, (dashed line) adjustment with a linear plot.

The first hyperpolarizability for dTMP was found to be $(1.67 \pm 0.15) \times 10^{-30}$ esu with a linear dependence of the HRS intensity with the square of the fundamental average power. Finally, experimental measurements for 2'-deoxyguanosine-5'-monophosphate (dGMP) are reported in Figure 5.

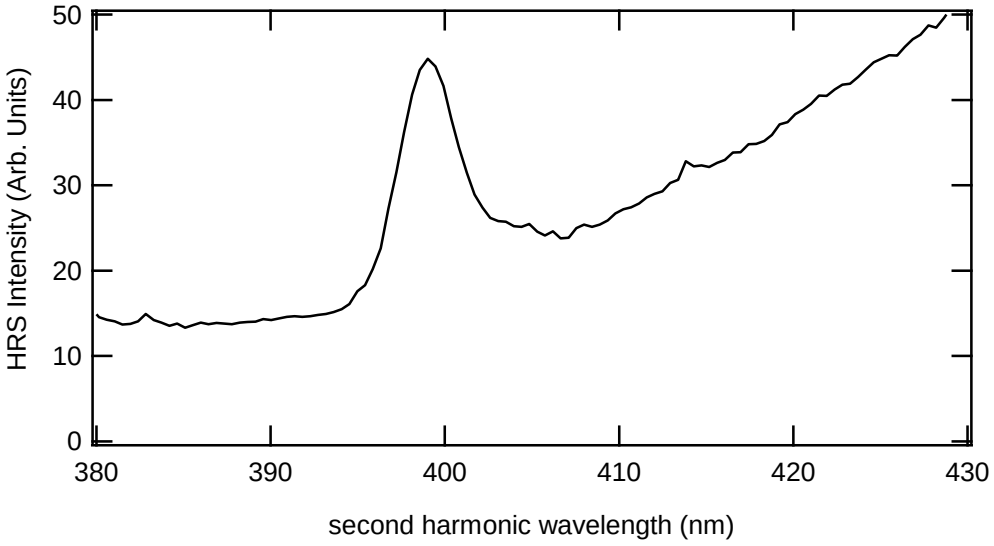

(a)

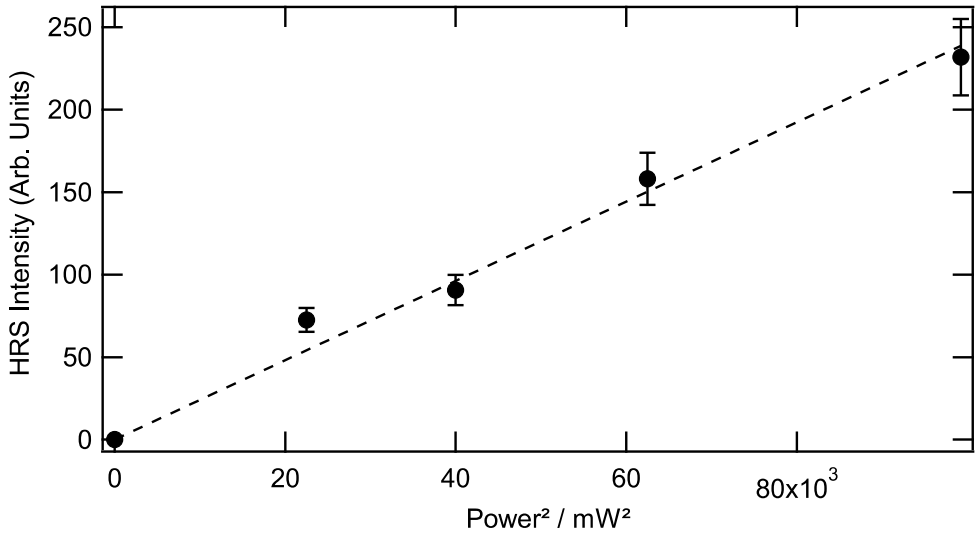

(b)

Figure 5 : (a) Spectrum of the HRS intensity at 400 nm of the 0.2 M dGMP aqueous solution for a 315 mW laser incident power for a 800 nm fundamental beam wavelength. (b) Dependence of the HRS intensity of the 0.2 M dGMP aqueous solution with the square of the fundamental average power, (markers) experimental data, (dashed line) adjustment with a linear plot.

A value of $(1.76 \pm 0.20) \times 10^{-30}$ esu is found for the first hyperpolarizability of dGMP again with the linear dependence of the HRS intensity with the square of the fundamental average power. Also of note, unlike dCMP and dTMP that do not present any marked multiphoton excited photoluminescence band, dGMP does just like dAMP, in an even more prominent way.

The measured four DNA nucleotides first hyperpolarizability values are very similar and close to the average value of about $(1.65 \pm 0.15) \times 10^{-30}$ esu. These values are of the same order of magnitude as the first hyperpolarizability of molecules with similar chemical structure.[28] It is therefore thought that, of the three components composing a nucleotide, the base entity accounts for most of the first hyperpolarizability whereas the phosphate and the sugar only provide distortions. Indeed, from the electron delocalization point of view, neither the phosphate group nor the sugar is expected to directly contribute significantly to the HRS signal. The charge delocalization on applying an external optical field is therefore expected to be mostly restricted within the base entity. Furthermore, there is no conjugation path to couple the base to the phosphate and the sugar groups. These groups, along with the substituting groups fixed on the aromatic rings can nevertheless be responsible for distortions in the symmetry of the overall nucleotide first hyperpolarizability. Also, because of the close similarity between the four nucleotides first hyperpolarizability values, the nature of the donor and acceptor groups attached to the base aromatic rings do not seem to play a dramatic role at the level of our sensitivity. Therefore, in order to investigate further the role of these side groups, polarization measurements were performed as well, see below.

Theoretical results. The static and dynamic electronic first hyperpolarizabilities of the four nucleotides were also determined in the water solvent using the DFT method at the B3LYP

level. All calculations were carried out with Gaussian 16 to solve the second-order Kohn-Sham equations.[29] The method presented here is formulated at the *ab initio* level within the framework of a continuous model of the solvent. The optimized geometric structures of the four nucleotides, see Figure 6, were obtained with the B3LYP/6–31G+(d) basis set as it is found to perform well for most geometries .[30]

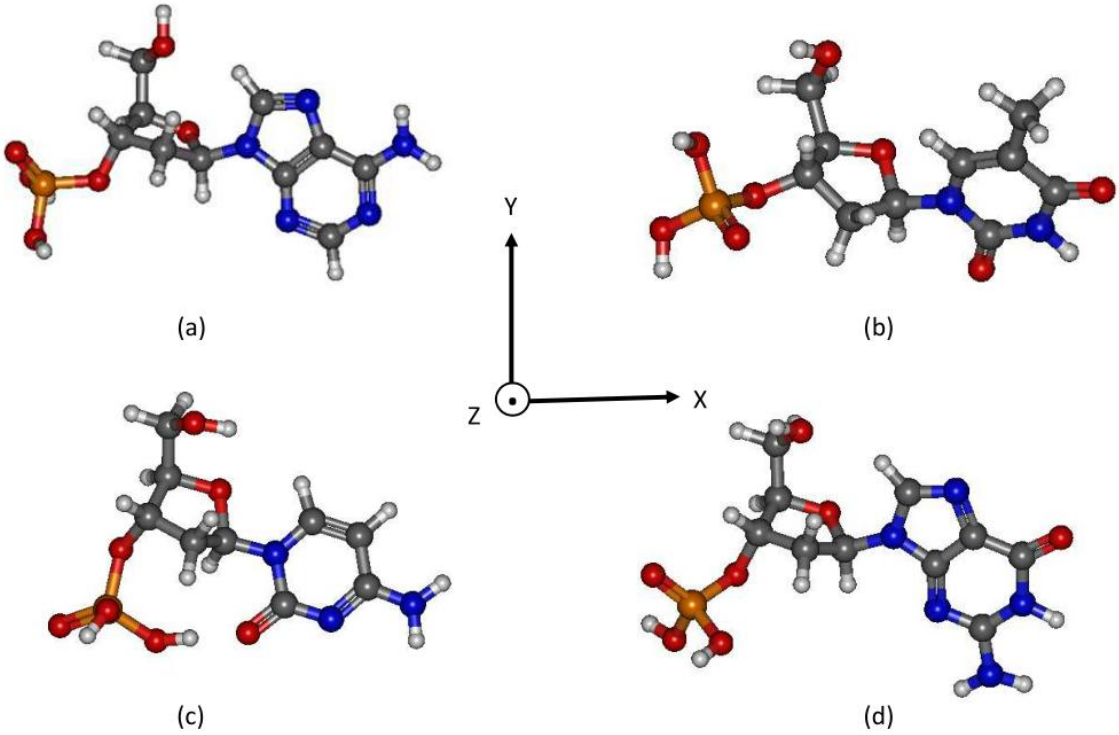

Figure 6 : Optimized geometry for the four nucleotides (a) dAMP, (b) dTMP, (c)dCMP and (d) dGMP. White balls represent H atom, red balls Oxygen atoms, blue balls Nitrogen atoms, grey balls Carbon atoms and Orange balls Phosphor atoms.

For the sake of clarity, the 2D representations of the four nucleotides are also displayed on Figure 7.

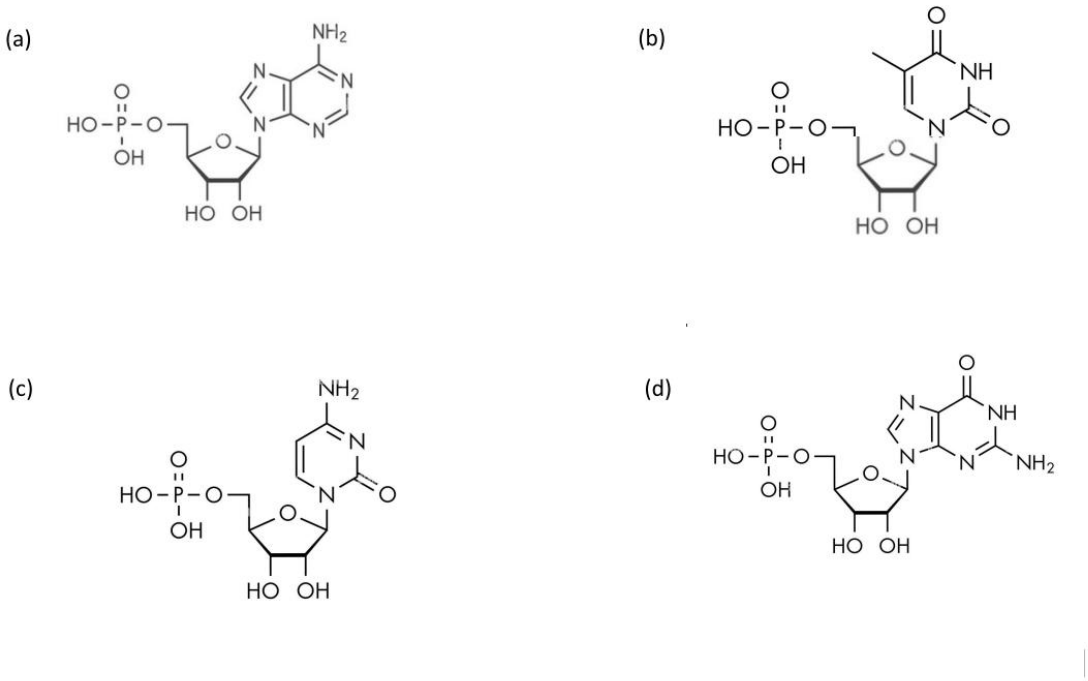

Figure 7 : 2D representations of the four nucleotides (a) dAMP, (b) dTMP, (c) dCMP and (d) dGMP

The geometry optimization calculations were performed in the gas phase and employed a polarizable continuum model (PCM) to take into account the solvent environment. The PCM using the integral equation formalism variant, as implemented in the Gaussian 16 package, was employed for this purpose. This model describes the molecular environment as a structureless polarizable continuum characterized, among other parameters, by its macroscopic dielectric permittivity $\varepsilon(\omega)$ which depends on the frequency ω of the applied electric field.[31, 32]

For all nucleotides, the differences between the molecular equilibrium geometries determined by the gas-phase and PCM calculations were checked to be negligible. The optimized (x, y, z) coordinates of each atom for all nucleotides are presented in the Supplementary Information file in Tables S1-S4. The static first hyperpolarizability values, $\beta(-2\omega; \omega,\omega)$ with

$\omega \rightarrow 0$, were calculated at the B3LYP/6-31+G(d) level. We selected the B3LYP functional and 6-31+G(d) basis set considering their satisfactory performances in the prediction of the response of electronic properties of organic compounds, reproducing adequately first-order hyperpolarizabilities obtained using high-level correlated ab-initio methods and larger basis sets.[29] The dynamic electronic first-order hyperpolarizability values for Second Harmonic Generation, $\beta(-2\omega; \omega,\omega)$, were calculated at the B3LYP/6-31+G(d) level as well in the $\hbar\omega$ range 0 – 0.057 a.u. where the latter energy corresponds to the wavelength of 800 nm, characteristic of the Ti:Sapphire laser used in this work. Table 1 lists the B3LYP/ 6-31+G(d) dipole moments and static electronic first hyperpolarizability tensor components β_{ijk} (i,j,k = x, y, z) in aqueous phase for the four nucleotides.

Table 1 : Static electronic first hyperpolarizabilities β_{ijk} in atomic units for the four nucleotides. Conversion factors from atomic units to esu is 1 a.u. $= 8.639 \times 10^{-3}$ esu and from atomic units to SI units is 1 a.u. $= 3.206361 \times 10^{-53}$ $C^3\,m^3\,J^{-2}$.

	β_{xxx}	β_{xxy}	β_{yxy}	β_{yyy}	β_{xxz}	β_{yxz}	β_{yyz}	β_{zxz}	β_{zyz}	β_{zzz}
dAMP	-258.9	-453.8	116.4	-72.9	-149.3	-64.3	4.4	52.6	-26.8	-13.3
dTMP	-66.7	-128.9	202.9	-188.1	-124.4	100.3	-38.9	14.7	-10.1	72.8
dCMP	-348.1	440.2	158.9	-422.2	-129.4	-10.6	141.7	50.7	33.1	-97.3
dGMP	-335.0	-193.0	86.6	564.5	7.59	-43.9	-228.6	102.2	43.6	32.3

In Eqs.(1)-(2) describing HRS experiments, first hyperpolarizabilities appear as $\langle\beta_i^2\rangle$, namely squared and averaged over all orientations due to the isotropy of the liquid phase. Hence, the relationship between $\langle\beta_i^2\rangle$ and the components of the molecular first hyperpolarizability tensor β_{ijk} depends on the polarization state of the fundamental and harmonic beams in order to select the adequate tensor elements in the macroscopic frame.[34] In our HRS experiments

the right-angle geometry is used. Therefore, in absence of polarization selection on the scattering direction, one has :

$$\beta_{HRS} = \sqrt{\langle \beta_{HRS}^2 \rangle} = \sqrt{\langle \beta_{XXX}^2 \rangle + \langle \beta_{ZXX}^2 \rangle} \quad (3)$$

using a geometry where the direction of propagation of the fundamental beam is OZ, the right-angle direction of collection OY and the vertical polarization of the fundamental beam OX. Assuming Kleinman symmetry allowing for the full permutation of the three indices of the tensor elements β_{ijk}, valid for compounds when working far from any resonance, the number of elements is reduced to 10 elements only as seen from Table 1. Then, first hyperpolarizability in the molecular and laboratory frame can be expressed with standard expressions.[34] The values for the dynamic first hyperpolarizability tensor elements of the four nucleotides are displayed below in Table 2.

Table 2 : Tensor elements of the dynamic first hyperpolarizability in atomic units of the four nucleotides evaluated at the λ value of 800 nm ($\hbar\omega$ =0.057 a.u). Conversion factors from atomic units to esu is 1 a.u. $= 8.639 \times 10^{-3}$ esu and from atomic units to SI units is 1 a.u. $= 3.206361 \times 10^{-53}$ $C^3 m^3 J^{-2}$.

Tensor components	dAMP	dCMP	dGMP	dTMP
β_{xxx}	-295.6	-198.5	-328.8	83.2
β_{yxx}	-283.9	214.9	-6.9	-117.5
β_{zxx}	-104.5	-97.6	-52.2	-54.0
β_{xyx}	-322.9	259.1	-24.2	-128.1
β_{yyx}	107.8	109.6	101.2	168.7
β_{zyx}	-35.6	-7.8	-7.7	94.3

β_{xyy}	150.3	106.4	105.2	177.9
β_{yyy}	-110.5	-320.4	383.4	-128.1
β_{zyy}	-23.8	93.7	-141.6	-38.4
β_{xzx}	-114.8	-110.0	-53.0	-55.2
β_{yzx}	-34.7	-6.5	-7.8	98.0
β_{zzx}	47.6	45.6	60.2	30.3
β_{xzy}	-28.3	-7.9	-7.4	106.4
β_{yzy}	-22.5	97.6	-143.5	-40.4
β_{zzy}	-14.9	26.9	25.1	-12.1
β_{xzz}	49.5	49.9	70.9	32.1
β_{yzz}	-19.6	30.7	29.4	-13.8
β_{zzz}	-17.6	-64.2	31.9	40.0

In the dynamic case, Kleinman symmetry is lost and 18 tensor elements survive out of the 27 elements due to the intrinsic permutation of the last two indices due to the frequency doubling process where the two fundamental photons are indistinguishable. The theoretical values of the first hyperpolarizability tensor elements in the laboratory frame were similarly expressed from the microscopic first hyperpolarizability tensor elements displayed in Table 2 with the standard expressions.[34]

In order to be compared with the tensor elements of the static and dynamic first hyperpolarizability obtained for the nucleobases we have given the tensor elements of the static and dynamic first hyperpolarizability within the dipole oriented reference frame, namely, with the z axis along the dipole moment. All the values are in the table S1-2 of the supplement information file.

In Table 3, the experimental and theoretical values in the laboratory frame of the first hyperpolarizabilities are then presented considering an incident fundamental wavelength fixed at 800 nm.

Table 3 : Values of the experimental and theoretical first hyperpolarizabilities $\beta_{HRS} = \sqrt{\langle \beta_{HRS}^2 \rangle}$ for the nucleotides and their associated nucleobases[22] in esu $\times\ 10^{-30}$.

Nucleotides	dAMP	dCMP	dGMP	dTMP
$\beta_{HRS}^{calculated}(800\ nm)$	2.16	1.77	1.96	1.60
$\beta_{HRS}^{exp}(800\ nm)$	1.70 ± 0.14	1.50 ± 0.12	1.76 ± 0.16	1.67 ± 0.15
Associated nucleobases	Adenine (A)	Cytosine (C)	Guanine (G)	Thymine (T)
$\beta_{HRS}^{calculated}(800\ nm)^{**}$	1.84	2.00	1.72	1.14
$\beta_{HRS}^{exp}(800\ nm)$	$< 1.82 \pm 0.10$	3.35 ± 0.21	*see note	2.99 ± 0.44

*No experimental value is reported in the literature due to its very low solubility.

** the experimental values of the nucleobase hyperpolarizabilities are extracted from Jonin et al.[22] while the theoretical values are calculated in the present study to take into account the solvent.

Experimentally and theoretically, all four nucleotides present very similar values for their first hyperpolarizability. As we can see in Table 3 though, the experimental values are systematically larger than the theoretical ones concerning the nucleobases and are smaller for the nucleotides except for dTMP for which the value is very closed.

Moreover, it has to be noticed that the nucleotides theoretical hyperpolarizability values are larger than that of the nucleobases indicating that the contribution of the sugar or the phosphate group is not completely negligible.

HRS resolved in polarization. In order to provide information about symmetry and ratios between first hyperpolarizability tensor elements, including their sign, we have also performed polarization – resolved HRS experiments. The HRS intensity measurements were

carried out as a function of the incident angle of polarization with the output polarization fixed, either vertical or horizontal. Results for the four nucleotides are displayed in Figure 8.

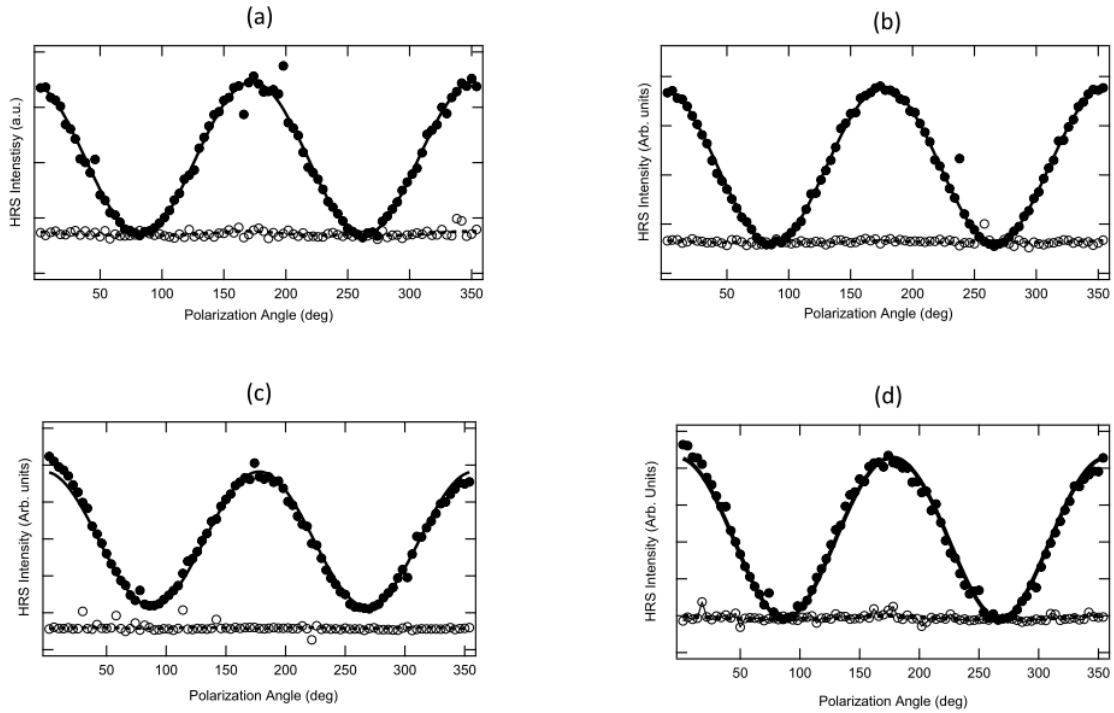

Figure 8 : Polarization resolved HRS intensity as a function of the fundamental beam angle of polarization (filled disks) vertically harmonic polarization and (empty disks) horizontally harmonic polarization for (a) dAMP, (b) dTMP, (c) dCMP and (d) dGMP.

For all the polarization graphs displayed, the polarization curves of the different solvents have been subtracted although noting that they were negligible except for dGMP and to a lesser extent dTMP. In all cases, the graphs display a well developed oscillatory behavior for the vertically polarized HRS intensity with maxima at 0, π and 2π fundamental beam polarization whereas the horizontally polarized HRS intensity is constant, independent of the fundamental beam polarization. The horizontally polarized HRS intensity also present intensities similar to the vertically polarized intensity at fundamental angles of polarization of

$\pi/2$ and $3\pi/2$. Only in the case of dCMP, these values are lower. HRS intensities for both vertical ($\Gamma = 90°, V$) and horizontal ($\Gamma = 0°, H$) polarization as a function of the fundamental beam polarization angle γ are given by [35] ;

$$I_{HRS}^{\Gamma} = a^{\Gamma}\cos^4(\gamma) + b^{\Gamma}\sin^2(\gamma)\cos^2(\gamma) + c^{\Gamma}\sin^4(\gamma) \quad (4)$$

In the electric dipole approximation and for fully incoherent HRS, the coefficients are linked together through the following relationships :

$$a^V + c^V = b^V \quad (5a)$$

$$2a^H = 2c^H = b^H \quad (5b)$$

$$c^V = c^H \quad (5c)$$

Hence, the above experimental data can be adjusted and the intensity parameters observed to follow Eqs.(5)(a)-(c) except for dCMP where Eq.(5c) appears broken. From this analysis, the main parameters to extract is the depolarization parameter defined as :

$$D^V = \frac{c^V}{a^V} = \frac{\langle\beta_{ZXX}^2\rangle}{\langle\beta_{XXX}^2\rangle} \quad (6)$$

The latter D^V parameter has been extracted for the four nucleotides and is tabulated in Table 4. The theoretical values obtained from the DFT calculations are also reported for comparison as these intensity parameters given in Eqs.(5)(a)-(c) can be expressed in terms of the first hyperpolarizability tensor elements in the laboratory frame.

Table 4: Experimental and theoretical values of the depolarization ratio for the four nucleotides. The four last columns indicate the theoretical values of the depolarization ratio for the nucleobases.

Depolarization Ratios	dAMP	dCMP	dGMP	dTMP	A	C	G	T
$D^V_{exp} = c^V/a^V$	0.19 ± 0.08	0.27 ± 0.05	0.17 ± 0.04	0.16 ± 0.04	-	-	-	-
$D^V_{Theory} = c^V/a^V$	0.32	0.64	0.32	0.28	0.25	0.62	0.23	0.45

In Table 4, experimental values of the depolarization ratio are closed to 0.2 except for dCMP that presents a slightly larger value. All experimental values follow the same trend albeit with larger values. This parameter D^V is associated with the symmetry of the molecular first hyperpolarizability. Within Kleinman relationship, a value close to 1/9 indicates a purely dipolar response whereas a value close to 2/3 indicates an octupolar response within the irreductible tensor reduction[32]. Besides, a molecule having a single element first hyperpolarizability tensor possesses a depolarization ratio of about 0.2.[36] Considering the above results in Table 2, and as seen from the theoretical values of the depolarization parameter, three comments can be made. First, the non vanishing value of all tensor elements in Table 4 indicates that the depolarization value close to 0.2 does not stem from a single dominating tensor element. Second, the dCMP polarization ratio is larger than that of the other nucleotides experimentally. Nevertheless, it remains rather small still indicative of a dipolar dominating symmetry. This further underlines the limit of the PCM description of the solvent.

Compared to dTMP, which has a geometry close to dCMP, the role of the amino group instead of the ketone group can be expected to play a role in the symmetry of the molecule leading to a change in symmetry. Nevertheless, the experimental results reveal a largely dipolar response for the four nucleotides. A similar behavior has notably been found in

compounds like 4-(4-dihexadecylaminostyryl)-N-methylpyridinium that exhibits a large delocalization along a single direction going through two aromatic rings and a styryl group bridging the two rings. Experimentally, the measured depolarization ratio was found to be equal to $D^V = 0.22 \pm 0.03$ in this case, with a single tensor element dominating the first hyperpolarizability tensor.[36]

Thus, it appears that the DFT calculations predict for all nucleotides a D^V parameter that agrees rather well with the observed experimentally values, albeit with a slightly larger value. These results confirm that the DFT computation of first hyperpolarizability tensor components is a suitable approach for these compounds dissolved in neat water or aqueous solutions. For dCMP, the experimentally observed value of D^V is larger than for the three other nucleotides, similarly to the theoretical values. However, the theoretical value close to 2/3 actually reveals an octupolar symmetry as opposed to a dipolar origin of the first hyperpolarizability. Likewise, the breaking of Eq.(5)(c) equality does not affect too much the depolarization ratio although the origin of the response should be given a closer scrutiny as this signature usually indicates the presence of coherent HRS contributions. It is therefore possible that dCMP is more sensitive to its nearby environment as compared to the three other nucleotides.

CONCLUSION

With the introduction of a sugar and a phosphate group, the nucleotides have a better solubility and can therefore all be studied within the same set of experiments. Comparison with the results on nucleobases is performed and shows nevertheless that the sugar and phosphate groups bring distortions, allowing for torsional movement around their axis, leading to rotational freedom of the bases around the nucleotide backbone.

In summary, we have built an advanced experimental setup with a high sensitivity for intensity and polarization-resolved hyper-Rayleigh scattering. This has allowed us to address the characterization of non-resonant small molecules where HRS intensity is rather weak and close to the neat solvent intensity.

The first hyperpolarizability of the four nucleotides was thus determined, with similar values closed of $(1.65 \pm 0.15) \times 10^{-30}$ esu. These values are of the same order of magnitude as those of similar molecules such as *pNA* or the four nucleobases.[22] It is also possible to perform polarization-resolved HRS measurements. This way, the depolarization ratio D^V can be determined as well. This parameter allows for the identification of the origin of the first hyperpolarizability tensor. In the present case, this origin is largely of dipolar nature as opposed to the octupolar one. These results have been compared with those predicted theoretically by DFT method and a good agreement is observed, both for the first hyperpolarizability magnitudes and the depolarization ratio except for dCMP suggesting a stronger environment effect for the latter one. In particular, these calculations highlight the distribution of the tensor over all its 18 elements, suggesting that the molecular symmetry does not obey too closely to a tabulated single symmetry. Subsequently, such experimental results can be used as a feedback to quantum chemical calculations applied for a computation of nonlinear optical properties of investigated molecules.

SUPPLEMENTARY MATERIAL : see supplementary material for the description of the HRS Photoluminescence separation by the spectral domain method, the Spatial Coordinates of minimized geometrical structures, the relationship between the tensor elements in the laboratory frame and the molecular frame, the Electronic first hyperpolarizabilities β_{ijk} within the dipole oriented reference frame and the dipole values of the nucleotides.

ACKNOWLEDGMENTS

M.D. and K.M. acknowledges funding from the National Science Centre in Poland within the Harmonia DEC/2016/22/M/ST4/00275 project and funding from the National Science Centre in Poland within the Opus UMO-2019/35/B/ST4/03280 project. All authors acknowledge funding from the PPN/BFT/2019/1/00030/U/0001 PHC POLONIUM project, cofunded by the Polish National Agency For Academic Exchange and Campus France.

REFERENCES

(1) I. Russier-Antoine, E. Benichou, G. Bachelier, C. Jonin, and P. F. Brevet, J. Phys. Chem. C **111**, 9044, 2007.

(2) S. Van Cleuvenbergen, I. Asselberghs, W. Vanormelingen, T. Verbiest, E. Franz, K. Clays, M. G. Kuzyk and G. Koeckelberghs, J. Mater. Chem. C, **2**, 4533, 2014

(3) K. Clays, A. Persoons, Phys. Rev. Lett.**,** ***66***, 2980-2983, 1991.

(4) G. J. T. Heesink, A, G, T Ruiter, N. F. van Hulst, B. Bölger, Phys. Rev. Lett., **71**, 999-1002, 1993.

(5) P. Kaatz, D. P. Shelton, Rev. Sci. Instr. **67**, 1438-1444, 1996.

(6) T. Verbiest, E. Hendrickx, A. Persoons, K. Clays, Nonlinear Optical Properties of Organic Materials V; Williams, D. J., Ed.; SPIE: Washington, **1775**, 206-212, 1992.

(7) T. W. Chui, K. Y Wong, J. Chem. Phys.**, 109**, 1391-1396, 1998.

(8) K. Clays, A. Persoons, Rev. Sci. Instrum.**, 65**, 2190-2194, 1994.

(9) S. Stadler, F. Feiner, C. Bräuchle, S. Brandl, R. Gompper, Chem. Phys. Lett., **245,** 292-296, 1995.

(10) M. Blanchard-Desce, S. Marder, M. Barzoukas, in Comprehensive Supramolecular Chemistry; Reinhoudt, D. N., Ed.; Elsevier: Oxford, **10**, 833-863, 1996.

(11) A. Sen, P. C. Ray, P.K Das, V. Krishnan, J. Phys. Chem.**, 100**, 19611, 1996.

(12) E. Hendrickx, A. Vinckier, K. Clays, and A. Persoons , J. Phys. Chem. **100**, 19672-19680, 1996.

(13) K. Clays, E. Hendrickx, M. Triest, T. Verbiest, A. Persoons, C. Dehu, J-L. Brédas, Science**, 262**, 1419-1422, 1993.

(14) P.K. Schmidt, G. W. Rayfield, Appl. Opt.**, 33**, 4286-4292, 1994.

(15) E. Hendrickx, A. Vinckier, K. Clays, A. Persoons, J. Phys. Chem.**, 100**, 19672-19680, 1996.

(16) E. Hendrickx, K. Clays, A. Persoons, C. Dehu, J.L Brédas, J. Am. Chem. Soc.**, 117**, 3547-3555, 1995.

(17) K. Clays, S. van Elshocht, A. Persoons, Opt. Lett.**, 25**, 1391-1393, 2000.

(18) K. Clays, S. van Elshocht, M. Chi, E. Lepoudre, A. Persoons, J. Opt. Soc. Am. B**, 18**, 1474-1482, 2001.

(19) A. Bansal, S. Kaushik, S. Kukreti, Front Genet. 2022, 13, 959258.

(20) M. Kaushik, S. Kaushik, K. Roy, A. Singh, S. Mahendru, M. Kumar, S. Chaudhary, S. Ahmed, S. Kukreti, Biochim. Biophys, 2016, 5, 388.

(21) N. Pandya, S.R. Bhagwat, A. Kumar, Biochim. Biophys. Acta. Rev. Cancer, 2021, 1876, 188594.

(22) Ch. Jonin, E. Salmon, and P-F. Brevet, J. Chem. Phys. **155**, 204306, 2021

(23) C. Jonin et al. Physical Chemistry Chemical Physics, 2023, in press

(24) K. Clays, A. Persoons, Phys. Rev. Lett., **66**, 2980 , 1991

(25) V. Rodriguez, J. Phys. Chem. C, **121**, 8510-8514, 2017.

(26) A. Rodriguez, M. Soljačić, J. D. Joannopoulos, and S. G. Johnson, Optics Express, **15**, 7303-7318, 2007.

(27) J. Duboisset, A. Deniset-Besseau, E. Benichou, I. Russier-Antoine, N. Lascoux, C. Jonin, F. Hache, M. C. Schanne-Klein, and P. F. Brevet, J. Phys. Chem. B, **117**, 9877-9881, 2013.

(28) J. Duboisset, G. Matar, I. Russier-Antoine, E. Benichou, G. Bachelier, Ch. Jonin, D. Ficheux, F. Besson, and P. F. Brevet, J. Phys. Chem. B, **114**, 13861–13865, 2010.

(29) M.J. Frisch, G.W. Trucks, H.B. Schlegel, G.E. Scuseria, M.A. Robb, J.R. Cheeseman, G. Scalmani, V. Barone, B. Mennucci, G.A. Petersson, H. Nakatsuji, M. Caricato, X. Li, H.P. Hratchian, A.F. Izmaylov, J. Bloino, G. Zheng, J.L. Sonnenberg, M. Hada, M. Ehara, K. Toyota, R. Fukuda, J. Hasegawa, M. Ishida, T. Nakajima, Y. Honda, O. Kitao, H. Nakai, T.

Vreven, J.A. Montgomery Jr., J.E. Peralta, F. Ogliaro, M. Bearpark, J.J. Heyd, E. Brothers, K.N. Kudin, V.N. Staroverov, R. Kobayashi, J. Normand, K. Raghavachari, A. Rendell, J.C. Burant, S.S. Iyengar, J. Tomasi, M. Cossi, N. Rega, J.M. Millam, M. Klene, J.E. Knox, J.B. Cross, V. Bakken, C. Adamo, J. Jaramillo, R. Gomperts, R.E. Stratmann, O. Yazyev, A.J. Austin, R. Cammi, C. Pomelli, J.W. Ochterski, R.L. Martin, K. Morokuma, V.G. Zakrzewski, G.A. Voth, P. Salvador, J.J. Dannenberg, S. Dapprich, A.D. Daniels, Ő. Farkas, J.B. Foresman, J.V. Ortiz, J. Cioslowski, D.J. Fox, Gaussian 09, revision A.02. Gaussian Inc., Wallingford, 2009.

(30) S. Prasenjit, J. Prakash Chandra,C. Swapan, J. Mol. Struc., **855,** 64–68, 2008.

(31) J. Tomasi and M. Persico, Chem. Rev. **94**, 2027. 1994.

(32) J. Tomasi, B. Mennucci, R. Cammi, Chem. Rev. **105**, 2999, 2005.

(33) B. Champagne and E. Botek, J. Chem. Phys. **122**, 114315, 2005.

(34) R. Bersohn, Y. H. Pao, and H. L. Frisch, J. Chem. Phys. **45**, 3184–3198, 1966.

(35) G. Revillod, J. Duboisset, I. Russier-Antoine, E. Benichou, G. Bachelier, C. Jonin and P.-F. Brevet, J. Phys. Chem. C, **112**, 2716–2723, 2008.

(36) J. Zyss and I. Ledoux Chem. Rev., **94**, 77-105, 1992